Monitoring ligand-dependent assembly of receptor ternary complexes in live cells by BRETFect

David Cotnoir-White[a,1], Mohamed El Ezzy[a], Pierre-Luc Boulay[a], Marieke Rozendaal[a], Michel Bouvier[a,b], Etienne Gagnon[a,c,1], and Sylvie Mader[a,b,d,1]

[a]Institute for Research in Immunology and Cancer, Université de Montréal, Montréal, QC H3T 1J4, Canada; [b]Département de Biochimie et Médecine Moléculaire, Université de Montréal, Montréal, QC H3T 1J4, Canada; [c]Département de Microbiologie, Infectiologie et Immunologie, Université de Montréal, Montréal, QC H3T 1J4, Canada; and [d]Centre de Recherche du Centre Hospitalier Universitaire de Montréal, Université de Montréal, Montréal, QC H2X 0A9, Canada

Edited by Pierre Chambon, Institut de Génétique et de Biologie Moléculaire et Cellulaire, Strasbourg, France, and approved January 19, 2018 (received for review September 24, 2017)

There is currently an unmet need for versatile techniques to monitor the assembly and dynamics of ternary complexes in live cells. Here we describe bioluminescence resonance energy transfer with fluorescence enhancement by combined transfer (BRETFect), a high-throughput technique that enables robust spectrometric detection of ternary protein complexes based on increased energy transfer from a luciferase to a fluorescent acceptor in the presence of a fluorescent intermediate. Its unique donor–intermediate–acceptor relay system is designed so that the acceptor can receive energy either directly from the donor or indirectly via the intermediate in a combined transfer, taking advantage of the entire luciferase emission spectrum. BRETFect was used to study the ligand-dependent cofactor interaction properties of the estrogen receptors ERα and ERβ, which form homo- or heterodimers whose distinctive regulatory properties are difficult to dissect using traditional methods. BRETFect uncovered the relative capacities of hetero- vs. homodimers to recruit receptor-specific cofactors and regulatory proteins, and to interact with common cofactors in the presence of receptor-specific ligands. BRETFect was also used to follow the assembly of ternary complexes between the V2R vasopressin receptor and two different intracellular effectors, illustrating its use for dissection of ternary protein–protein interactions engaged by G protein-coupled receptors. Our results indicate that BRETFect represents a powerful and versatile technique to monitor the dynamics of ternary interactions within multimeric complexes in live cells.

bioluminescence resonance energy transfer | ternary complexes | nuclear receptors | G protein-coupled receptors | heterodimers

The need to interrogate multimeric protein complex formation in live cells is crucial for our understanding of a multitude of cellular processes, including signal transduction and transcriptional regulation. Ternary complexes can be detected by fluorescence resonance energy transfer (FRET), based on sequential transfer between three fluorophores in a three-color or triple-FRET assay (1, 2). However, this approach suffers from constraints due to photobleaching and contaminating cross-excitation requiring spectral unmixing, typically yielding low signal output and a restricted dynamic range. The need for an advanced microscopy setup has also limited implementation in high-throughput screens. Bioluminescence resonance energy transfer (BRET) assays do not require use of fluorescence excitation, reducing the need for compensation in the acceptor channel due to cross-excitation. The enhanced cell survival also extends the potential duration of dynamic follow-up. BRET interrogates interactions between two protein partners, but combination with either a protein complementation assay (PCA) or FRET has been used to a limited extent to detect ternary complexes (3, 4). Reconstitution of a green fluorescent protein or a luciferase from separate fragments in a PCA (5, 6) enables combination with BRET for spectrometric detection of complexes involving three proteins but can affect the kinetics of assembly and stability of complexes as well as introduce conformational constraints, leading to a high rate of false negative results (3). Carriba et al. (4) developed an approach termed "sequential resonance energy transfer," based on sequential transfer of energy from a donor to an intermediate by BRET and subsequently to an acceptor by FRET, to measure heteromeric interactions between more than two neurotransmitter receptors. However, potential shortcomings include signal contamination, necessitating resolution by spectral unmixing, and inefficient coupling between chromophores, reducing the output signal, limiting the use of serial resonance energy transfer (SRET) as a versatile, high-throughput–amenable spectrometric detection method for heteromeric complexes.

To overcome the limitations of current ternary complex detection methods, we developed a RET assay that entails the use of an intermediate fluorescence protein tailored to ensure a strong increase in output signal when the ternary complex is formed while minimizing artifactual signals. We termed this method "BRET with fluorescence enhancement by combined transfer" (BRETFect) and demonstrate using several examples that it reliably enables spectrometric detection of ternary complex formation in live cells without the need for spectral unmixing. We validated this approach for the study of homodimers formed by the estrogen receptors ERα or ERβ, which function as dimeric ligand-dependent transcription factors that recruit a variety of cofactors via two transcriptional activation

Significance

Many biological processes, including signal transduction pathways and gene expression regulation, require the assembly of multisubunit protein complexes in a temporally coordinated fashion. However, approaches to studying the dynamics and properties of multimeric complex assembly currently remain limited. We have developed a method to monitor assembly of trimeric complexes in live cells, using a specific combination of bioluminescence- and fluorescence-based energy transfer. We illustrate the potential of this technology to reveal ligand-activated assembly of ternary protein complexes involving nuclear receptors or G protein-coupled receptors (GPCRs) and their effectors or regulators. We show that this methodology uniquely enables the functional characterization of nuclear receptor heterodimers and the demonstration of corecruitment of effector proteins to a GPCR.

Author contributions: D.C.-W., E.G., and S.M. designed research; D.C.-W., M.E.E., and M.R. performed research; M.B. contributed new reagents/analytic tools; D.C.-W., P.-L.B., M.B., E.G., and S.M. analyzed data; and D.C.-W., E.G., and S.M. wrote the paper.

The authors declare no conflict of interest.

This article is a PNAS Direct Submission.

[1]To whom correspondence may be addressed. Email: david.cotnoir-white@umontreal.ca, etienne.gagnon@umontreal.ca, or sylvie.mader@umontreal.ca.

This article contains supporting information online at www.pnas.org/lookup/suppl/doi:10.1073/pnas.1716224115/-/DCSupplemental.

Published online February 27, 2018.

domains, AF1 and AF2 (7–10). ERs mediate estrogenic effects in a wide range of physiological processes and pathologies, including breast cancer (7, 11). ERα and ERβ have distinct functional properties, including differential roles in estrogen-induced breast cancer cell growth (11–14) and in response to synthetic antiestrogens used in the clinic to block estrogen signaling (15, 16). ERα and ERβ have overlapping tissue-specific expression patterns and can form heterodimers when coexpressed, but the patterns of specific cofactor recruitment by heterodimers in the presence of various ER ligands remain underexplored due to a lack of suitable assays (12). Using BRETFect, we revealed that the ERα partner in heterodimers is sufficient to trigger recruitment of an ERα AF1-specific cofactor domain in the presence of agonists, or of small ubiquitin-like modifier (SUMO) modification marks in the presence of pure antiestrogens, and demonstrated that receptor-selective ligands induced recruitment of common cofactors to heterodimers with intermediate potencies. Finally, we documented the versatility of BRETFect by detecting ternary complexes formed by the G protein-coupled receptor (GPCR) V2R and its effectors.

Results

Design of BRETFect for the Detection of Ternary Complex Formation Through Combined Energy Transfer. BRETFect relies on the use of a donor (D)–intermediate (I)–acceptor (A) relay system where the acceptor can receive energy either directly from the donor or indirectly via the intermediate in a combined transfer at the population level (Fig. 1*A*). The intermediate is chosen such that it can act as a relay to increase the total energy that can potentially be transferred from the donor to the acceptor, by transferring energy from parts of the emission spectrum of the donor that are inefficient for direct excitation of the acceptor. Renilla luciferase II (RLucII) (17) converting coelenterazine h (coel-h) has a very broad bioluminescence emission spectrum (400 to 600 nm; Fig. 1*B*), reflecting a wide range of energetic states upon oxidative conversion of the substrate. Energy transfer between RLucII and a yellow-shifted GFP, for instance Venus (18, 19), occurs because of overlap between the emission spectrum of the donor and the excitation spectrum of the acceptor (Fig. 1*B*), resulting in a reduction in RLucII emission in the wavelengths overlapping with the Venus excitation spectrum and an increase in signal output at wavelengths corresponding to Venus fluorescence emission. However, less than half of the emission spectrum of RLucII/coel-h overlaps with the Venus excitation spectrum (Fig. 1*B*, blue and yellow dotted lines, respectively), indicating that many of the energetic states arising from coel-h oxidation are not compatible with RET.

A similar observation is made when considering the spectral overlap between RLucII and another BRET partner, monomeric TFP1 (mTFP1) (Fig. 1*C*, blue and cyan dotted lines, respectively). Interestingly, mTFP1 (20) and Venus do not compete for resonant energy transfer, due to the minimal overlap between their excitation spectra (Fig. 1*D*, cyan and yellow dotted lines, respectively). This suggests that mTFP1 can act as an energy relay between RLucII/coel-h and Venus for the portion of the emission spectrum that is less favorable for direct transfer to Venus (i.e., the 400- to 460-nm window) (Fig. 1*D*). Indeed, energy transfer from RLucII/coel-h to mTFP1 would lead to an emission peaking around 492 nm, which represents more favorable energetic states for resonant energy transfer to Venus (Fig. 1*D*). Thus, in the luciferase population, each RET event corresponds to emission of energy at a single specific wavelength between 400 and 600 nm and transfer to either the intermediate (400 to 460 nm) or the acceptor (470 to 520 nm) (Fig. 1*D*). Hence, the entire width of the donor emission spectrum is used for either direct transfer to the acceptor or indirect transfer via successive RET events from the donor to the intermediate to the acceptor (Fig. 1*A*, *Right* and Fig. 1*D*).

To measure the combined energy transfer from D to A directly and from D to A through I, we detect the total transfer output (TTO), namely wavelengths compatible with emission from A (Venus), versus the combined transferable output potential (CTOP), namely wavelengths compatible with energy transfer to A from either D or I (Fig. 1 *B–D*). For TTO measurements, we opted for filters that enable detection of Venus emission with minimal spectral overlap with mTFP1 (LP550 nm). Though the overall signal detection from Venus at those wavelengths is less optimal than with the BP530/20 filter set, this choice minimizes the detection of mTFP1 emission, eliminating a potential source of confounding signals. On the other hand, CTOP is measured by detecting signal emission in the range that encompasses both RLucII/coel-h and mTFP1 emission spectra (BP485/40 nm). Selecting these wavelengths, rather than the usual RLucII/coel-h BRET donor detection channel (BP400/70 nm), has

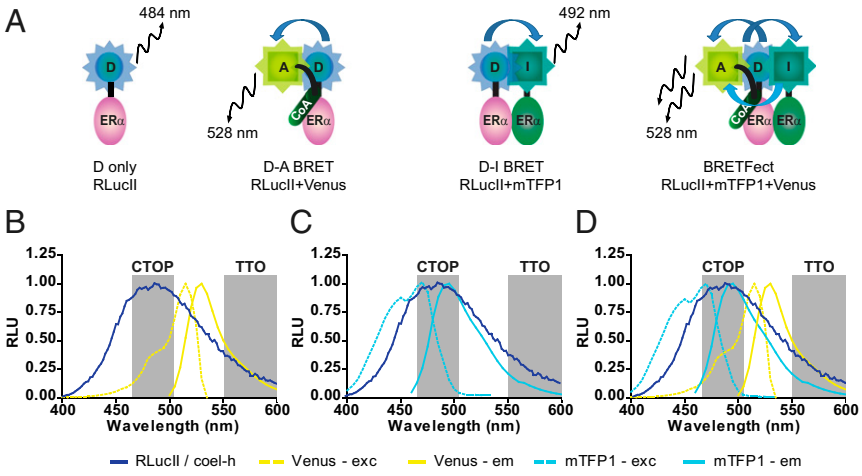

Fig. 1. BRETFect design. (*A*) Description of energy transfer between a donor tagged with RLucII (D), an intermediate tagged with mTFP1 (I), and an acceptor tagged with a YFP (A) in the presence of two or three partners. In the example illustrated, ERα is fused with RLucII or mTFP1 to generate D and I, respectively, and a coactivator is fused with Venus to generate A. (*B–D*) Analysis of donor RLucII (dark blue line), intermediate mTFP1 (pale blue line), and acceptor Venus (yellow line) excitation (exc) and emission (em) spectra (dotted or full line, respectively) after direct stimulation of luciferase or fluorophores in HEK293T cells expressing each construct independently. The emission and excitation peaks were standardized to a maximum of 1.00. Shaded areas represent the filter windows used for detection in BRETFect assays. RLU, relative light unit.

the advantage of preventing the calculation of false positive A/D signal ratios that may result from quenching of RLucII/coel-h emission by mTFP1 without subsequent transfer to Venus. Therefore, the formation of a ternary complex between D, I, and A should result in an increase in the overall BRET ratios between CTOP and TTO at the population level without the need for spectral unmixing. This increase is due to the additional energy absorbed and then transferred by I and should be greater than the sum of net BRET ratios in each binary condition, D + I (which should be negligible) and D + A (reflecting transfer without an intermediate), using the same CTOP and TTO detection channels (Fig. 1*A*).

Because of these considerations, BRETFect (Fig. 1*A*) differs from SRET (Fig. S1*A*) in terms of design and basic principles of energy transfer within ternary complexes. Importantly, BRETFect does not posit a strictly sequential transfer between D, I, and A for the detection of ternary complex formation. While the sequential transfer hypothesis is central to SRET, we note that it appears unlikely to always be upheld in SRET[1], which uses a YFP such as Venus and DsRed as fluorophores (4), because of the significant overlap between the excitation spectra of these fluorescent proteins (Fig. S1 *B* and *C*). This suggests that I and A would compete for direct energy transfer from D if both interactions can take place simultaneously within the ternary complex. Binary complexes between D and A may thus artificially increase the ternary signal. In addition, use of DsRed in this setup may lead to the formation of aberrant fusion protein complexes due to the propensity of DsRed to tetramerize (21). Also, in SRET[2], which associates GFP2 and a YFP such as Venus as I and A, respectively (4), the significant overlap between the emission spectra of GFP2 and Venus (Fig. S1*D*) may cause an overestimation of the ternary signal in the absence of proper spectral unmixing (see also below).

In BRETFect, use of mTFP1 and of a YFP (e.g., Venus, Topaz, or eYFP, which share similar excitation and emission peaks; Fig. S1*B*) as I and A, respectively, minimizes the overlap in the excitation spectra of I and A and reduces contamination in the acceptor channel by the intermediate (TTO detection: LP550 nm), while enabling detection of most of the intermediate emission in the donor channel due to the coincidence of the mTFP1 and RLucII/coel-h emission spectra (CTOP detection: BP485/40 nm) (Fig. 1*C*). This more accurately accounts for the total energy available for transfer to the acceptor and for its resulting emission output. The choice of mTFP1 in combination with RLucII/coel-h as a donor is key to the efficacy of BRETFect. This is due to the superior brightness of coel-h (Fig. S1*E*) and the high quantum yield of mTFP1 (Fig. S1*B*), enabling a robust signal output as well as efficient use of the entire width of the RLucII/coel-h emission spectrum for transfer to the acceptor YFP. Of note, use of a different intermediate fluorophore such as mTagBFP2 (22), whose excitation profile is not compatible with energy transfer from RLucII/coel-h (Fig. S1*F*), can provide a useful negative control.

Validation of BRETFect as a Method to Detect Ternary Complex Formation Between ERα Homodimers and a Coactivator Peptide in Live Cells. To validate the applicability of BRETFect to the analysis of ternary complex formation in live cells, we monitored the recruitment to ERα homodimers of an LXXLL coactivator motif (CoA), which mediates interaction of several cofactors with the AF2 transcriptional activation domain of nuclear receptors (23). Recruitment of such motifs to ERα in the presence of the natural ER agonist 17β-estradiol (E2) has been previously detected in live cells using BRET or FRET (24, 25). BRET can also monitor ER dimer formation (26, 27). To detect complexes formed between an ERα homodimer and the CoA motif by BRETFect, we fused the ERα protein to RLucII or to mTFP1, yielding the donor and intermediate, respectively, and used CoA fused to Venus as the acceptor (Fig. 1*A*). HEK293T cells were transiently transfected to express binary and ternary combinations of D, I, and A in the presence of E2 to stimulate CoA recruitment by ERα. The emission profiles were plotted after normalization according to the area under the curve to illustrate how the energy is redistributed during RET. In the absence of a BRET partner, conversion of coel-h by ERα-RLucII (D) produced a broad emission peak (Fig. 2 *A*–*C*, dark blue line) with the expected maximum at 484 nm (Fig. S1*B*). Addition of CoA-Ven (D + A) led to significant changes in the RLucII emission spectrum in the presence of E2 (Fig. 2*A*, compare green and dark blue lines). The marked decrease in signal intensity at wavelengths lower than 525 nm is compatible with quenching by the acceptor (Venus), and the increase at wavelengths greater than 525 nm is compatible with Venus emission, indicating energy transfer between D and A through CoA recruitment by agonist-bound ERα. Similarly, when ERα-RLucII and ERα-mTFP1 were cotransfected, the observed decrease in emission around 464 nm and the shift in the maximal emission peak from 484 to 492 nm are compatible with quenching of RLucII and with mTFP1 fluorescence emission, respectively, indicative of RET between D and I due to ERα homodimerization (Fig. 2*B*, light blue line vs. dark blue line). Finally, cotransfection of all three tagged components (D + I + A) led to a drop in emission around 464 nm and a significant increase in emission around 528 nm compared with the spectral profiles from D + A, indicating formation of the ternary complex (Fig. 2*C*, yellow line compared with green line). To better illustrate the effect of the intermediate on signal output, we subtracted the normalized emission profile of the binary complex (D + A) from the emission profile of the ternary complex (D + I + A) (Fig. 2*D*). These results illustrate a decrease in emission signal centered at 464 nm (black line), overlapping with the excitation profile of mTFP1 (blue line), and a corresponding emission signal increase centered around 528 nm, coinciding with the fluorescence emission profile of Venus (yellow line), strongly suggesting combined energy transfer within the ternary complex. To directly validate RET between mTFP1 and Venus within the ternary complex, we performed a standard FRET experiment in the absence of coel-h. Results confirmed efficient energy transfer between ERα-mTFP1 and CoA-Ven following E2 treatment (Fig. S2*A*). Taken together, these observations validate the predicted pattern of energy transfer and amplification by the intermediate mTFP1, and show that ternary complex formation can be monitored using BRETFect.

BRETFect Is a Robust and Easy-to-Implement Spectrometric Method for Ternary Complex Detection. Next, we compared BRETFect with SRET[2] for the detection of ternary complexes between ERα homodimers and the CoA motif in the presence of E2, which induces complex formation, or of antiestrogens, which do not (28). In both setups, RLucII was fused to ERα. Based on the original description of SRET[2] (4), we used RLucII/coelenterazine 400a (coel-400a) as a donor and fluorescent proteins GFP2 and Venus as intermediate and acceptor, respectively (Fig. S1*D*). In parallel, we investigated a modified SRET[2] approach using mTFP1 instead of GFP2 as an intermediate. For both types of assays, nontagged ERα (α-notag) was used as control for the intermediate (D + A condition) to ensure similar complex stoichiometry, and unfused Venus (Ven) was cotransfected in the D + I condition to control for random collisions (Fig. 2*E*).

In the SRET[2] assays, cotransfection of the donor ERα-RLucII (α-Luc) together with either ERα-GFP2 or ERα-mTFP1 (α-GFP or α-TFP) as intermediates and unfused Venus led to the generation of significant BRET signals in the SRET acceptor channel (530 nm) in all treatment conditions, but particularly with the antiestrogen ICI182,780 (ICI; Fig. 2*E*), in agreement with previous observations (26). However, the significant signals detected in these control D + I binary conditions represent contaminating signals in the ternary complex SRET assays (see also below). On the other hand, in BRETFect, the control binary condition (D + I) resulted in low signal in all ligand conditions (Fig. 2*E*), highlighting minimal contaminating signals from the

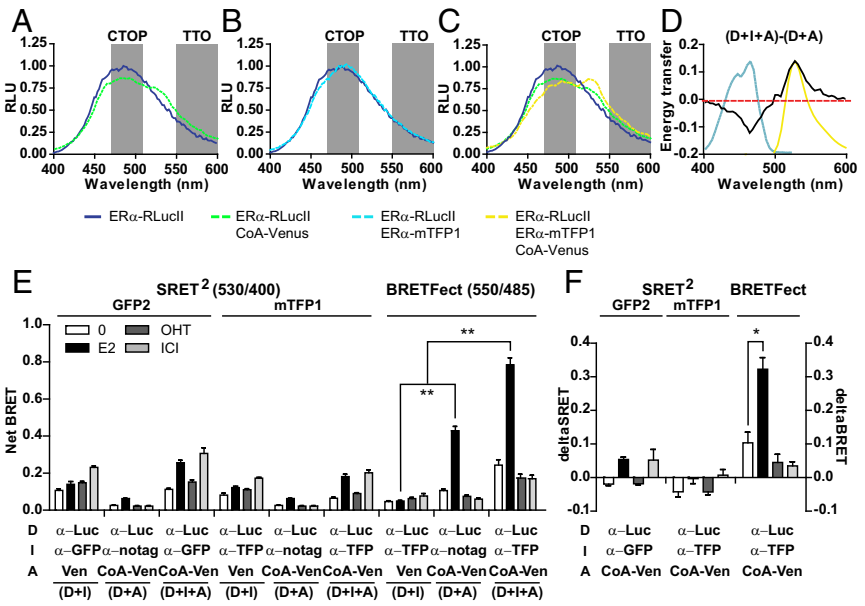

Fig. 2. BRETFect monitors ternary complex formation between ERα dimers and coactivators in live cells. (*A–C*) Spectral analyses of luminescence emission by HEK293T cells expressing fusion proteins ERα-RLucII, ERα-mTFP1, and/or CoA peptide-Venus (CoA-Ven), or unfused versions of Venus or of ERα, and treated with E2 for 45 min. Values are the average of three biological replicates. (*D*) BRET signals for donor–acceptor (D + A) were subtracted from the BRET signals for the ternary condition (D + I + A) across the wavelength spectrum. The intermediate absorption spectrum (blue line) and the acceptor emission spectrum (yellow line) are superimposed. (*E*) Net BRET signals (530/400 nm in SRET^2 and 550/485 in BRETFect) in cells expressing the indicated fusion proteins and/or unfused controls after treatment with ligands (1 μM) for 45 min. Coel-400a was used in SRET^2 vs. coel-h in BRETFect. (*F*) Delta SRET and delta BRETFect were calculated as [(A + I + D) − (D + I) − (D + A)] from data in *E*. All graphs were prepared from at least three biological replicates, and error bars represent the SEM. Statistical significance was analyzed by ANOVA with a Bonferroni post hoc test. $*P < 0.01$, $**P < 0.001$.

intermediate in the TTO detection window (LP550 nm; Fig. 1 *C* and *D*). Instead, mTFP1 emissions, which peak at 494 nm, are recaptured in the CTOP channel in BRETFect(BP485/40 nm) (Fig. 1 *C* and *D*) but not in SRET(BP400/70 nm). As expected from the BRETFect design, the D + A binary condition produced a robust BRET signal upon treatment with E2, while antiestrogens 4-hydroxytamoxifen (OHT) and ICI suppressed the basal signal, consistent with their inhibitory effect on AF2 function (Fig. 2*E*). A similar pattern of BRET signals was detected in the D + A conditions using both SRET^2 assays, albeit with greatly reduced intensities, indicating weak but specific direct transfer from D to A despite the sequential transfer assumption (4).

Cotransfection of all ternary complex partners using BRETFect conditions led to a significant amplification of the net BRET ratios following E2 treatment, but not in the presence of antiestrogens OHT and ICI (Fig. 2*E*). This is compatible with increased energy transfer at the population level in the ternary complex formed specifically in the presence of the agonist E2 due to transfer from the intermediate, mTFP1, to the acceptor by FRET (Fig. S2*A*), in addition to direct transfer from donor to acceptor (Fig. 2*A*). Replacing the intermediate fluorophore mTFP1 with mTagBFP2, yielding ERα-mTagBFP2 (α-BFP2), failed to increase the overall energy transfer to the acceptor compared with the unfused receptor (ERα) or the absence of intermediate (none) (Fig. S2*B*). As mTagBFP2 is very inefficient at accepting energy from luciferase in the presence of coel-h (Fig. S1 *B* and *F*), this clearly indicates that the increase in signal output in the BRETFect approach is dependent on combined energy transfer. In contrast, neither SRET^2 assay led to significant signal amplification in the E2 condition compared with signals in the presence of antiestrogens OHT or ICI (Fig. 2*E*), which prevent CoA recruitment and therefore ternary complex formation, indicating that SRET failed to detect specific ternary complex formation under our experimental conditions.

The difference between BRETFect and SRET is further showcased using a differential BRET calculation (delta BRETFect or delta SRET) obtained by the subtraction of the binary condition net BRET signals (D + I and D + A) from the ternary condition signals (D + I + A) for each treatment (Fig. 2*F*). The delta BRETFect was, as expected, enhanced by E2, while OHT and ICI reduced it significantly. However, both SRET^2 assays yielded minimal signals after compensation for contaminating emissions, and no clear differential signal between the agonist E2 and the antiestrogens OHT and ICI could be obtained (Fig. 2*F*). Several factors may account for the failure to reliably monitor ternary complex formation using SRET^2. As discussed above, a likely contributing factor is the overlap between the emission spectra of GFP2 (I) and Venus (A), the signal observed in the ternary D + I + A condition (yellow curve) being at least in part confounded by that of the D + I binary condition (blue curve) (Fig. S2*C*). In addition, GFP2 has a weaker extinction coefficient (the capacity to receive energy from the donor) and a poorer quantum efficiency (the capacity to transmit the received energy as resonant energy) compared with mTFP1 (Fig. S1*B*). However, replacement of GFP2 by mTFP1 in SRET^2 did not lead to significant improvement in specific signal detection (Fig. 2 *E* and *F*). Other limitations include the use of coel-400a in SRET^2, which also likely contributes to weaker signal-to-noise ratios, as coel-h has increased brightness (Fig. S1*E*) and leads to a better overlap between RLucII emission and mTFP1 excitation (Fig. 1*C*). Third, use of the TTO and CTOP detection channels in BRETFect both minimizes signals from the intermediate in the acceptor detection channel and detects more appropriately the transferable energy from the donor or the intermediate, thus helping to reduce confounding signals.

To further characterize the specificity of ternary complex detection with BRETFect, we titrated amounts of A or I in the D + I + A condition. As expected, BRET levels were dependent on the concentration of CoA-Ven and could be saturated under all treatments, as expected for specific interactions (Fig. S2 *D* and *E*). Furthermore, BRET signals were also amplified in a concentration-dependent manner by ERα-mTFP1, but not untagged ERα, demonstrating the role of the intermediate in signal potentiation (Fig. S2 *F* and *G*). The specificity of this signal amplification was further demonstrated by the use of a non–ERα-interacting peptide (mutCoA), which yielded only residual BRET signal (Fig. S2*H*). Further, the non–ERα-interacting nuclear receptor Nurr77 or the dimerization-deficient ERα mutant L507R fused to mTFP1 both failed to amplify BRET (Fig. S2*H*). Together, these results validate that BRETFect enables specific and robust detection of the agonist-induced formation of ternary complexes between ER dimers and cofactors.

BRETFect Reveals the Patterns of Ligand-Dependent Recruitment of Coactivators by ER Heterodimers. We used BRETFect to characterize the specific patterns of protein–protein interactions by

ERα–ERβ heterodimers and increase our understanding of their biological properties. Both ERα and ERβ recruited CoA-Ven in an E2-induced and OHT-repressed manner in BRET assays (Fig. 3*A*, D + A conditions). Note that similar levels of expression of the ERα and ERβ fusion proteins were achieved (Fig. S3*A*), and that CoA-Venus was also expressed similar to the unfused Venus control (Fig. S3*B*). Addition of ERα-mTFP1 to either ERα-RLucII or ERβ-RLucII potentiated the BRET signal for recruitment of CoA-Ven in the basal and E2-induced but not in the OHT conditions (Fig. 3 *A* and *B*, D + I + A conditions), indicating that CoA is recruited in a similar manner to ER homodimers and heterodimers. On the contrary, ligand-dependent recruitment of p160 cofactors by the AF1 domain has been reported to take place with ERα but not ERβ (29). As expected, E2 induced recruitment of the AF1-interacting domain (AF1ID) of the p160 cofactor SRC1 fused to the YFP Topaz to ERα, but not ERβ, in BRET assays (Fig. 3*C*, D + A conditions). In addition, OHT acted as a partial agonist for recruitment of AF1ID to ERα, consistent with previous reports (29). Cotransfection of ERα-mTFP1 with ERα-RLucII (D + I + A condition) significantly potentiated the signal in the presence of E2, while cotransfection of ERβ-mTFP1 with ERβ-RLucII led to signal potentiation under basal conditions but no further increase by E2 (Fig. 3 *C* and *D*), in keeping with previous observations of ligand-independent cofactor recruitment by the ERβ AF1 domain (30). Interestingly, coexpression of ERα-mTFP1 with ERβ-RLucII also significantly potentiated energy transfer between ERβ and the AF1ID in the presence of E2 (Fig. 3 *C* and *D*), indicating that ERα maintains its capacity for ligand-induced recruitment of the AF1ID coactivator domain within heterodimers. Similar results were obtained in bone U2OS cells, demonstrating applicability of the method to different cell backgrounds (Fig. S3 *C* and *D*).

Use of protein motifs or domains as acceptors is often resorted to in BRET when working with large proteins, due to the need to express high protein levels in titration curves. Here we have investigated the size limitation for the amplification potential of BRETFect compared with standard BRET using full-length cofactors. We tested the capacity of BRETFect to monitor recruitment to ER dimers of coregulators spanning a variety of protein sizes, i.e., PPARGC1A/PGC1α (803 aa), LCoR (433 aa), and NR0B2/SHP1 (257 aa) (9, 10, 31). As expected, recruitment of these cofactors (fused to Topaz) to ERα-RLucII in regular BRET was agonist-induced in all cases (Fig. S3*E*). In addition, LCoR was also recruited in the presence of OHT. On the other hand, ICI did not induce ternary complex formation for any of the cofactors tested (Fig. S3*E*), as previously reported. Similar results were obtained by FRET between ERα-mTFP1 and the various cofactor fusions (Fig. S3*G*). Finally, the D + I + A conditions led to a ligand-dependent signal potentiation compared with the control binary conditions (Fig. S3 *E* and *F*), demonstrating its use for enhancing the detection of interactions between nuclear receptors and acceptor proteins of varying sizes (up to about 90 kDa). However, potentiation was stronger for smaller proteins (Fig. S3*F*), in keeping with the lower expression levels of large fusion proteins. In addition, the size of the acceptor may also affect energy transfer efficiency via altered positioning or orientation of the fluorophore with respect to the donor or intermediate, as in classical two-partner BRET.

The Pure Antiestrogen Fulvestrant Selectively Induces SUMOylation of ERα-Containing Dimers. ERα SUMOylation was previously shown to contribute to the enhanced transcriptional suppression of ERα by antiestrogens of the selective estrogen receptor down-regulator (SERD) class such as ICI182,780, also known as fulvestrant, compared with the selective estrogen receptor modulator (SERM) OHT (32). However, the role of ERα dimerization in ICI-induced SUMOylation and the specificity of this modification for ERα vs. ERβ have not been characterized. In a BRETFect assay, ICI induced BRET signals between SUMO3-eYFP and ERα-RLucII (D + A) after 120 min of treatment, indicating a marked increase in ERα SUMOylation (Fig. S4*A*). Cotransfection of ERα-mTFP1 (D + I + A) strongly potentiated the signal in the presence of ICI (Fig. 4*A* and Fig. S4*A*), indicating that ERα homodimers are SUMOylated. However, no signal potentiation was observed in the presence of ICI with a SUMO mutant incapable of covalent attachment to substrates (SUMO1G; Fig. 4*B*). Signal potentiation by I upon ICI treatment was also dependent on a dimerization-competent receptor partner, as it was not observed with dimerization-deficient ERL507R (Fig. 4*B*). Absence of SUMOylation of ERL507R

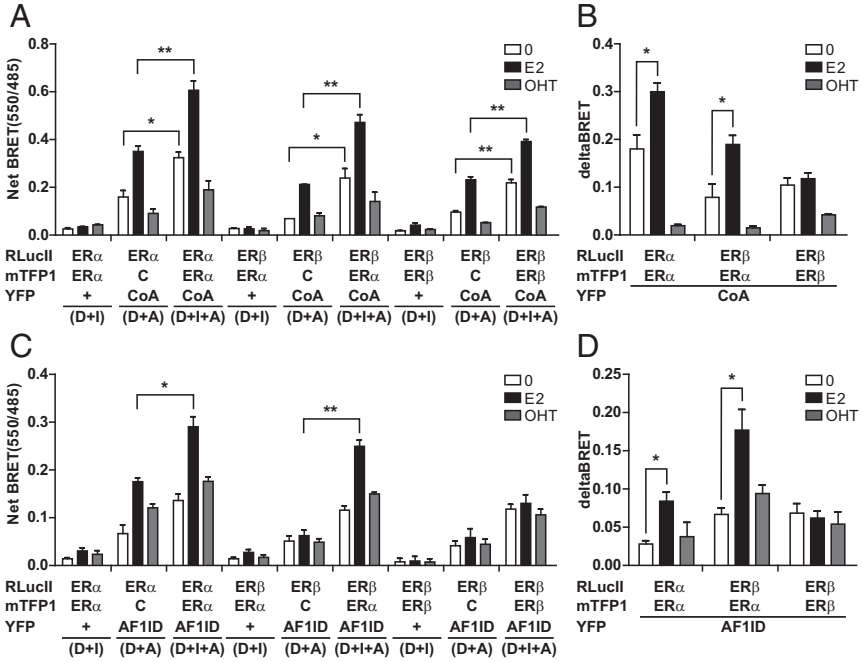

Fig. 3. ERα–ERβ heterodimers recruit AF1ID in a ligand-dependent manner. (*A*) BRETFect analysis of ligand-dependent recruitment of CoA peptide (CoA) to ERα or ERβ homodimers or heterodimers. HEK293T cells expressing ERα/β-RLucII, ERα/β-mTFP1, and the CoA peptide fused to Venus or unfused controls (C, unfused ERα; +, unfused Venus) were treated with ligands (1 μM) for 45 min. (*B*) Delta BRET calculations from BRETFect assays in *A*. (*C*) BRETFect analysis of ligand-dependent recruitment of AF1ID to ER dimers. Cells expressing ERα/β-RLucII, ERα/β-mTFP1, and/or AF1ID fused to Topaz were treated as in *A*. (*D*) Delta BRET calculations from BRETFect assays in *C*. All graphs were prepared from at least three biological replicates, and error bars represent the SEM. Statistical significance was analyzed by ANOVA with a Bonferroni post hoc test. $*P < 0.01$, $**P < 0.001$.

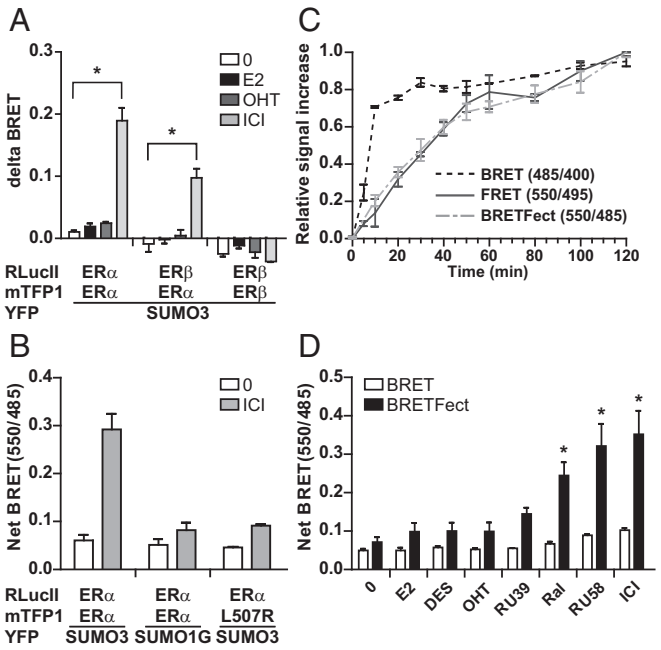

Fig. 4. SERD-induced SUMOylation of ER dimer entities requires the presence of one ERα partner. (*A*) Delta BRET values were calculated from BRETFect assays (Fig. S4*A*) performed in HEK293T cells expressing vectors for ERα/β-RLucII, ERα/β-mTFP1, and/or SUMO3 fused to eYFP and treated for 2 h with 1 μM E2, OHT, or ICI182,780. (*B*) The nonconjugatable SUMO1G mutant and the monomeric ERα(L507R) mutant were used as specificity controls in BRETFect assays in *A*. (*C*) Kinetic analysis of binary and ternary complex formation between ERα-RLucII, ERα-mTFP1, and SUMO3-eYFP after treatment with ICI (1 μM). BRET ratios (485/400) were calculated from cells treated with coel-400a, BRETFect ratios (550/485) from cells treated with coel-h, and FRET ratios (550/495) from light-excited cells. Relative signal increases were plotted according to time after ICI addition. (*D*) Comparative detection of ligand-induced SUMOylation by BRET or BRETFect in HEK293T cells expressing ERα-RLucII and SUMO3-eYFP in the presence or absence of ERα-mTFP1 and treated for 2 h with ligands (1 μM). Graphs were prepared from three biological replicates, and error bars represent the SEM. Statistical significance compared with untreated controls was analyzed by ANOVA with a Bonferroni post hoc test. *$P < 0.01$.

was verified by Western analysis (Fig. S4*B*). On the other hand, ICI did not detectably induce SUMOylation of ERβ in a standard BRET (D + A) (Fig. S4*A*) and cotransfection of ERβ-mTFP1 did not potentiate the BRET signal obtained with the ERβ-RLucII fusion protein in the presence of any ligand (D + I + A) (Fig. 4*A* and Fig. S4*A*). Western blot analyses confirmed the ICI-dependent SUMOylation of GFP-fused ERα but not ERβ (Fig. S4*C*).

Interestingly, the coexpression of ERα-mTFP1 with ERβ-RLucII (D + I + A condition) led to a significant signal potentiation in the presence of ICI through BRETFect, although to a lower degree than with ERα-RLucII (Fig. 4*A* and Fig. S4*A*), suggesting that SUMO molecules are present on heterodimers as well as ERα homodimers. Reduction of ERα SUMOylation (but not of unmodified ERα levels) upon coexpression of ERβ could be confirmed using Western blotting (Fig. S4*D*). Similar BRETFect results were obtained in U2OS bone cells (Fig. S4*E*). Together, our results indicate that heterodimer formation reduces the capacity of ICI to induce ERα SUMOylation but that SUMO marks can be detected on heterodimers, whether through de novo addition on heterodimers or monomer exchange between ERα homo- and heterodimers.

Next, we exploited the capacity of BRETFect to measure in parallel the three potential binary interactions within ternary complexes to investigate the kinetics of SUMOylation vs. those of receptor dimerization within the first 100 min after ICI treatment in cells transiently transfected to express all three BRETFect components (D + I + A). Energy transfer between ERα monomers fused to RLucII or mTFP1 (D + I) was monitored at different times after ICI addition by measuring 485/400 BRET ratios (using coel-400a rather than coel-h); to determine ICI-dependent SUMOylation kinetics on ERα, we monitored FRET signal ratios between ERα-mTFP1 and SUMO3-eYFP (550/495, I + A) after excitation at 420 nm; finally, to determine ICI-dependent SUMOylation kinetics on ERα dimers, we monitored BRETFect signal ratios using coel-h and the TTO and CTOP detection channels (550/485, D + I + A). We plotted all data obtained from these parallel assays onto a single graph, where we normalized the signal ratios to the maximal signal obtained. A sharp increase in BRET(485/400) signal ratios was observed within the first 10 min upon addition of ICI (Fig. 4*C*), compatible with rapid effects of ICI on receptor dimerization and/or conformational change. On the other hand, gradual increases in FRET(550/495) and BRETFect(550/485) signal ratios were observed. Together, these results indicate that progressive SUMOylation occurs on preformed ERα homodimers (Fig. 4*C*). In addition, these results also illustrate the multiplexing capacity of BRETFect assays and their usefulness in dissecting the contribution of individual interaction partners in ternary complex assembly in real time.

We have previously observed that some SERM molecules with reduced partial agonist properties such as raloxifene (Ral) can induce low levels of SUMOylation compared with SERDs (32). Here, we used BRETFect to test whether signal amplification compared with BRET enables a greater sensitivity in the detection of SUMO marks. ICI and the antiestrogen RU58,668 (RU58), which both belong to the SERD class of antiestrogens, induced comparable strong SUMOylation signals in our BRETFect assay (three- to fourfold increase compared with background). In contrast, agonists E2 and diethylstylbestrol (DES) or the SERM OHT did not significantly induce SUMOylation using the same assay. However, a marked and statistically significant ($P = 0.0094$) increase in SUMOylation was detected in the presence of Ral compared with untreated samples. Interestingly, this increase was minimal and did not reach significance under the same conditions in the standard BRET assay (Fig. 4*D*). This clearly highlights the increased sensitivity of BRETFect and its applicability to the detection of rare ternary complexes. Induction of SUMOylation by Ral is in agreement with results obtained by Western analysis (32) and correlates with the improved antiestrogenic profile of Ral compared with OHT in HepG2 cells, an experimental model for the agonist activity of SERMs (26, 32).

Receptor-Selective Ligands Induce Coactivator Recruitment by Heterodimers with Intermediate Potencies. Receptor-selective agonists such as the ERα-specific agonist propylpyrazole triol (PPT) or ERβ-selective agonist diarylpropionitrile (DPN) have been developed to independently target each receptor and dissect their individual roles (33–35). Although these ligands are permissive for heterodimer formation (27, 36), their impact on the activity of these heterodimers has not been characterized. BRETFect assays are particularly suitable to assess this question in live transfected cells via the monitoring of CoA-Venus recruitment by different combinations of ERα and ERβ fused to RLucII or mTFP1. As expected, PPT, like E2, led to a dose-dependent recruitment of CoA-Ven by ERα-RLucII in BRET assays (Fig. 5*A*, yellow and black curves). These signals were increased at all drug concentrations by addition of an ERα-mTFP1 intermediate partner (Fig. 5*A*, blue and red curves), demonstrating the recruitment of CoA to ERα homodimers in the presence of ERα-binding ligands.

Similarly, addition of either ERβ-selective DPN or non-selective E2 led to a dose-dependent recruitment of CoA-Ven by ERβ-RLucII in BRET assays (Fig. 5*B*, yellow and black curves), and these signals were increased at all drug concentrations by addition

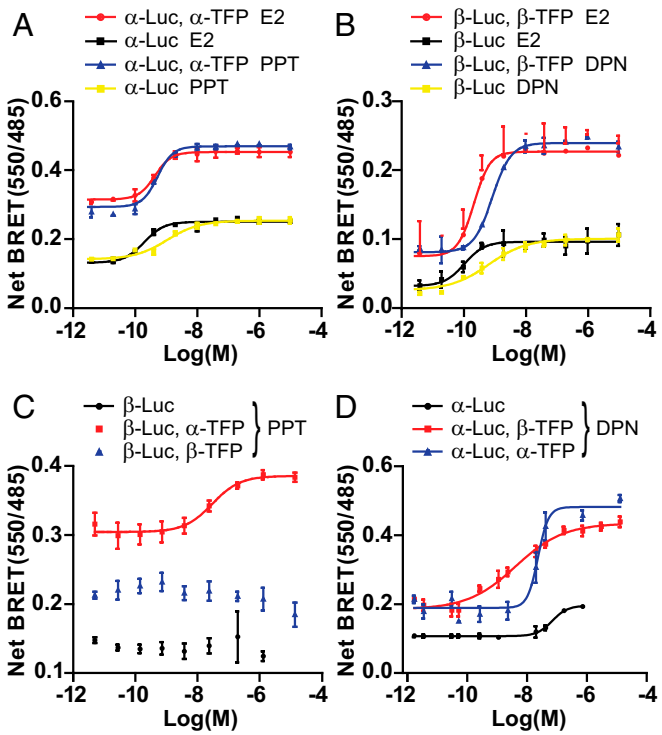

Fig. 5. Activation of ERα–ERβ heterodimers by selective ligands. HEK293T cells expressing the indicated constructs together with the CoA-Ven expression vector were treated with ligands (4×10^{-12} to 1×10^{-5} M) for 45 min. (*A* and *B*) BRETFect analysis of ternary complex formation induced by E2 (*A* and *B*, black and red lines) compared with either PPT for ERα homodimer (*A*, blue and yellow lines) or DPN for ERβ homodimer (*B*, blue and yellow lines). (*C*) BRETFect analysis of ERα-specific ligand PPT on ERβ homodimer (blue points) and ERα/ERβ heterodimer (red line). (*D*) BRETFect analysis of ERβ-selective ligand DPN on ERα homodimer (blue line) and ERα/ERβ heterodimer (red line). Standard BRET assays with ERβ-Luc (*C*, black points) or ERα-Luc (*D*, black line) are also shown. All graphs were prepared from three biological replicates, and error bars represent the SEM. Curves were generated by nonlinear regression analysis of the data.

of an ERβ-mTFP1 intermediate partner (Fig. 5*B*, blue and red curves), demonstrating the recruitment of CoA to ERβ homodimers in the presence of ERβ-binding ligands.

On the other hand, no increase in CoA recruitment was observed as expected in BRET using ERβ-RLucII upon addition of different concentrations of ERα-specific PPT (Fig. 5*C*, black points) or in the presence of cotransfected ERβ-mTFP1 (Fig. 5*C*, blue points). However, PPT stimulated coactivator recruitment by ERβ-RLucII in the presence of cotransfected ERα-mTFP1 (Fig. 5*C*, red line), indicating activation of ERα–ERβ heterodimers by PPT. Interestingly, PPT was less potent for coactivator recruitment by the ERα–ERβ heterodimer than by the ERα homodimer (EC_{50} 28 nM vs. 0.55 nM; Table S1), suggesting positive allosteric effects between liganded homodimeric partners. Assays performed with the SRC1 receptor-interacting domain (RID), which contains multiple CoA-like interacting motifs, indicated that PPT also promoted recruitment of the entire RID to the heterodimer with lower potency compared with ERα homodimers (Fig. S5*A* and Table S2).

Conversely, addition of different concentrations of ERβ-selective DPN led to recruitment of CoA-Ven by ERα-RLucII as monitored by BRET assays (Fig. 5*D*, black curve), and cotransfection of ERα-mTFP1 potentiated this signal (Fig. 5*D*, blue curve), demonstrating activation of ERα by DPN, albeit with EC_{50}s 20-fold higher than with ERβ homodimers (Table S1). However, cotransfection of ERβ-mTFP1 led to an increase of BRETFect signal at lower doses of DPN (Fig. 5*D*, red curve), reflecting activation with intermediate EC_{50} values compared with ERα and ERβ homodimers (Table S1). The recruitment of CoA-Ven in the presence of ERβ-mTFP1 at DPP concentrations that do not activate ERα-RLucII (black curve, low nanomolar range) validates the formation of a ternary complex between CoA-Ven and a receptor heterodimer. Similar results were obtained with the SRC1 RID (Fig. S5*B* and Table S2). Further, ligand titration curves indicate that the recruitment capacity for CoA-Ven to α-Luc was reduced by half in the heterodimer with PPT, which binds only ERα, compared with E2 or DPN (Fig. S5*C*). This observation is compatible with in vitro structural studies illustrating a stoichiometry of one CoA motif per receptor molecule within dimers in live cells (37, 38). Taken together, these results reveal that heterodimers can achieve cofactor recruitment in the presence of both types of ER-selective agonists, although with lower potencies compared with the targeted homodimer. Moreover, the trimeric ERα–ERβ–CoA BRETFect assay, with a *Z* factor of 0.528 (Fig. S5*D*), was found to be sufficiently robust to be applicable to high-throughput screens of small-molecule libraries modulating CoA recruitment by ER heterodimers for research or therapeutic purposes (39).

BRETFect Is a Versatile Technique to Study Ternary Complex Formation. To assess whether BRETFect could be applied to other types of protein complexes, we monitored the formation of ternary complexes involving G protein-coupled receptors. Constitutive dimerization of many GPCRs has been demonstrated using a diversity of approaches, including coimmunoprecipitation, protein complementation assays, FRET, and BRET (40, 41). Engagement of downstream effectors, including G proteins and β-arrestin, by GPCR dimers upon agonist stimulation has been revealed for the chemokine receptor CXCR4 by bimolecular fluorescence complementation combined with BRET (42) and using synthetic dimerizing ligands for dimers of the V2-vasopressin receptor (V2R) (43). To directly monitor the formation of a ternary complex between V2R dimers and β-arrestin 2 (βArr2) upon activation with the agonist arginine vasopressin (AVP), we developed a BRETFect assay using V2R-RLucII, V2R-mTFP1, and βArr2-Venus. As expected, AVP promoted a significant increase in BRET in the control binary condition (D + A) (Fig. S6*A*). However, a significant enhancement of signal output was observed in the D + I + A condition only in the presence of AVP (Fig. 6*A* and Fig. S6*A*). These results are consistent with current models of association of βArr2 with a dimeric receptor following activation by AVP.

Assessing energy transfer between V2R and βArr2 in the absence or presence of AVP as a function of time indicated that the AVP induction occurred very rapidly (less than 10 min) either in standard BRET(550/485) between V2R-RLucII and βArr2-Venus (Fig. S6*B*, light blue squares compared with light blue dots) or in FRET(550/485) between V2R-mTFP1 and βArr2-Venus (Fig. S6*C*, green squares vs. green dots). Addition of the intermediate (V2R-mTFP1) potentiated the BRET(550/485) signal in the presence of AVP (Fig. S6*A*, dark blue squares vs. light blue squares) but not in its absence (Fig. S6*B*, dark blue dots vs. light blue dots), reflecting the need for AVP for recruitment of βArr2 to a V2R homodimer. Calculation of the differential BRET signals in the presence vs. the absence of AVP illustrates the similitude in the kinetics of induction of ternary interactions assessed by BRETFect (Fig. 6*B*, dark red curve) vs. the binary interactions assessed in control BRET conditions without intermediate (Fig. 6*B*, light red curve) or in FRET between V2R-TFP and βArr2-Venus (Fig. 6*B*, black line), compatible with the recruitment of βArr2 to assembled V2R homodimers. Note that, as in nuclear receptor BRETFect assays (see above and Fig. S2*F*), BRET signals in the ternary condition increased in a saturable dose-dependent manner with the amount of

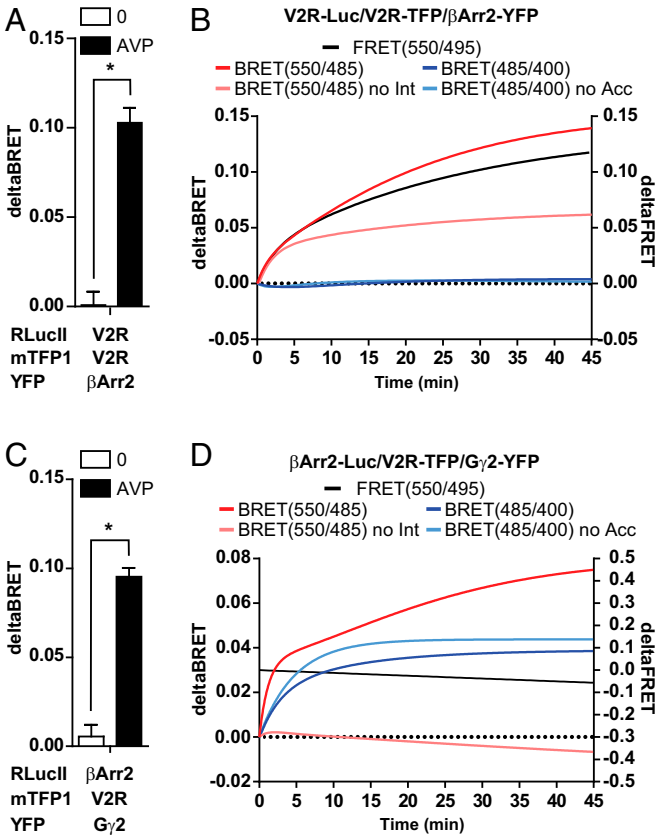

Fig. 6. BRETFect detects formation of ternary complexes containing the GPCR V2R receptor and downstream effectors. (*A*) BRETFect assays in HEK293T cells expressing V2R fused to RLucII (donor), beta-arrestin2 fused to Venus (acceptor), and mTFP1-tagged V2R (intermediate). Delta BRET values were calculated from net BRET signals in Fig. S6*A*. (*B*) Time course of AVP induction of βArr2 recruitment to V2R in standard BRET (light red), BRETFect (dark red), or FRET (black) assays. Energy transfer between V2R molecules in a dimer is also shown in the presence (dark blue) or absence (light blue) of acceptor βArr2-Venus. Values represent the AVP-induced increase in signal over nontreated cells, calculated from data in Fig. S6 *B* and *C*. (*C* and *D*) BRETFect assays in HEK293T cells expressing βArr2-RLucII (donor), Gγ2-Venus (acceptor), and V2R-mTFP1 (intermediate). (*C*) Delta BRET values were calculated from net BRET signals in Fig. S6*E*. (*D*) Time course of AVP-induced recruitment of βArr2 to Gγ2 in the presence of V2R (BRETFect; dark red) or its absence (standard BRET; light red). Kinetics of FRET between V2R-mTFP1 and Gγ2-Venus (black line) and of βArr2 recruitment to V2R in the presence (dark blue) or absence (light blue) of acceptor Gγ2-Venus are also shown. Values represent the AVP-induced increase in signal over nontreated cells, calculated from data in Fig. S6 *F* and *G*. Graphs were prepared from three biological replicates, and error bars represent the SEM. Statistical significance was analyzed by ANOVA with a Bonferroni post hoc test. *$P < 0.001$. No Int, no intermediate; No Acc, no acceptor.

cotransfected intermediate component V2R-mTFP1 (Fig. S6*D*) and were entirely dependent on the presence of AVP, as previously observed (Fig. 6*A*). Finally, using coel-400a, we also monitored the energy transfer between donor and intermediate components (BRET485/400; red curves in Fig. S6*B*). Our results show a lack of impact of AVP on energy transfer between two V2R molecules, and a lack of influence of the coexpression of the acceptor βArr2-Venus on these measurements in the presence or absence of AVP (Fig. 6*B*, dark and light blue lines).

We next used BRETFect to assess whether a ternary complex can be formed between V2R (fused to mTFP1), βArr2 (fused to RLucII), and the G-protein γ-subunit (Gγ2; fused to Venus), as recently proposed by Thomsen et al. (44). In the absence of the intermediate V2R-TFP, AVP (1 μM) did not induce changes in BRET signal between βArr2 and Gγ2 (D + A) at 20 min (Fig. S6*E*) nor at any time point (Fig. S6*F*, light blue squares vs. light blue dots). The observed AVP-insensitive background may be explained by corecruitment of βArr2 and Gγ2 at other GPCRs expressed in HEK293T cells (Fig. S6*E*). In contrast, coexpression of V2R-TFP led to a large AVP-dependent potentiation of the BRETFect signal at 20 min, indicative of ternary complex formation (Fig. 6*C*). Ternary complex formation was observed very rapidly after AVP addition (Fig. 6*D*, dark red curve; see also Fig. S6*F* for individual BRET measurements). This was confirmed by parallel monitoring of donor-to-intermediate transfer by BRET(485/400), which enables the detection of AVP-dependent transfer of energy between βArr2 and V2R at the same time points in the presence or absence of Gγ2-Venus (Fig. 6*D*, blue lines). On the other hand, energy transfer between V2R-mTFP1 and Gγ2-Venus detected by FRET(550/495) was essentially stable in time and independent of the presence of AVP (Fig. 6*D*, black line and Fig. S6*G*), consistent with a stable association of these two components during the assays. Together, these results confirm observations of a precoupling of GPCRs to G proteins (45–48) and of maintained association between V2R and Gγ2 upon AVP-dependent βArr2 recruitment (44).

Taken together, observations generated using our BRETFect approach provide direct confirmation of the formation of ternary complexes between GPCRs, G proteins, and β-arrestins upon ligand stimulation, as recently proposed using a combination of biochemical and binary BRET approaches (44). Importantly, these results highlight the versatility of BRETFect as a robust method to detect ternary complex formation in live cells.

Discussion

BRETFect is a RET assay for the detection of ternary protein complexes in live cells, based on combined transfer at the population level between a donor protein and an acceptor or an intermediate protein. The intermediate (herein mTFP1) was chosen based on its capacity to relay emissions from the lower to the upper wavelengths in the RLucII emission spectrum for improved transfer to the acceptor, while minimizing emission in the acceptor detection channel. The resulting effect of the presence of the intermediate partner in a ternary complex is increased energy transfer to the acceptor and, consequently, a net increase in acceptor/donor BRET signal compared with dimeric conditions, or to control intermediate proteins (unfused partner or fusion with mTagBFP2). The choice of detection channels for the combined transferable output potential from both the donor and intermediate (CTOP; BP485/40 nm) and for the acceptor (TTO; LP550 nm) not only improves overall detection of ternary complex formation but suppresses the need for spectral unmixing. Thus, ternary complex formation can be evaluated by calculation of a delta BRET signal between the conditions when all three partners are present simultaneously and control conditions where the donor is present only with the intermediate or the acceptor. Similar to other RET approaches, a limitation of BRETFect can be the lack of detection of an interaction (false negative) due to steric hindrance from the fused fluorophores or to their inappropriate orientation. This problem can be mitigated by adding tags at different ends of the proteins or within loops (49). In addition, linkers can be used between the fused proteins to minimize steric hindrance (50).

The BRETFect approach was successfully applied to the study of ligand-induced assembly of complexes between estrogen receptors and transcriptional cofactors. A strong potentiation of the BRET signal for the interaction between a molecule of ERα and cofactor motifs, domains, or entire proteins was observed when an additional ER molecule linked to mTFP1 was cotransfected in the presence of agonists but not upon treatment with an antagonist, validating the approach for the detection of a ternary complex between ER dimers and cofactors. Similar results were observed when monitoring formation of covalent

complexes formed between ERα dimers and modifier proteins such as SUMO1/3. Note that signal increase upon addition of the intermediate is not due simply to changes in the affinity of the donor for its interaction partners (YFP fusion proteins) in the presence of the intermediate (ERα or ERβ fused to mTFP1), as equal amounts of WT ERα unfused to the intermediate fluorophore (mTFP1) were transfected in the control D + A conditions. In addition, fusing ERα to mTagBFP2, which cannot act as an intermediate, generated the same results as unfused ERα, indicating the need for energy transfer via the intermediate for signal potentiation. Further, nondimerizing receptors fused to mTFP1 highlighted the specificity of this potentiating effect for an intermediate fusion protein forming a ternary complex with the donor and acceptor. Finally, use of noninteracting acceptor fusion proteins (mutCoA or SUMO1G) confirmed that signal amplification does not result simply from emission of the intermediate in the acceptor detection channel.

The terminal acceptor proteins used in our BRETFect assays (eYFP, Venus, and Topaz) are all yellow-shifted derivatives of GFP and hold the potential for forming low-affinity dimers, particularly under increased local concentrations due to fusion to transmembrane proteins or obligate oligomers (19). Although this may potentially alter the stoichiometry or stability of ternary complex assembly due to increased protein crowding or steric hindrance, this should not affect the signal amplification induced by the mTFP1-fused partner within the complex. Indeed, mTFP1 cannot form low-affinity dimers with the YFP variants used in our assays, nor can it relay the resonant energy to more than one YFP per transfer. In addition, monomeric YFP versions obtained through introduction of the mutation A206K can be used to address stoichiometry or stability issues (19).

BRETFect differs from SRET in its design, based on combined vs. sequential transfer, reflected in different selections of donor, intermediate, and acceptor proteins, as well as of the detection channels for spectrometric evaluation of complex formation. When a SRET^2 setup was used, contaminating signals from the intermediate in the acceptor channel and the lack of efficient amplification upon addition of the third partner resulted in weak and aberrant BRET signals in the ternary condition, failing to demonstrate differential CoA recruitment by an ER dimer in the presence of an agonist (E2) vs. antagonists (OHT, ICI). This could not be resolved by subtraction of the signals obtained for the two pairwise dimeric complexes (D + I and D + A), and would likely require spectral imaging and linear unmixing (51), hampering applications to high-throughput screening.

We then validated the use of the BRETFect approach by assessing recruitment of cofactor/regulator proteins by estrogen receptor homodimers in a ligand-modulated manner, for example, the AF2-interacting CoA peptide, AF1ID, and SUMO molecules, the latter two having a different interaction pattern with ERα and ERβ homodimers. We further used BRETFect to characterize the capacity of ERα–ERβ heterodimers to interact with these proteins in live cells. Importantly, BRETFect revealed that ERα–ERβ heterodimers partially preserve ERα-specific patterns of protein–protein interactions. The observed ligand-induced recruitment of AF1ID by heterodimers as well as ERα homodimers, but not ERβ homodimers, is consistent with and provides a mechanism for previous observations of the dominance of the ERα AF1 region in heterodimers in reporter assays (52). In addition, BRETFect detected modification of heterodimers as well as ERα homodimers, but not ERβ homodimers, by SUMOylation in the presence of SERDs. BRETFect thus provides a unique approach to dissect ligand-modulated recruitment of cofactors or modifier proteins to heterodimers.

Discovery of ligands regulating formation of specific nuclear receptor (NR) complexes (e.g., here ERα–ERβ heterodimers vs. ERα or ERβ homodimers) represents an important pharmacological opportunity to modulate NR action in a more targeted manner (12, 53), but necessitates the availability of appropriate assays. Here we show that BRETFect reveals novel aspects of ERα–ERβ heterodimer function, namely their capacity to recruit CoA AF2-interacting motifs in the presence of either ERα- or ERβ-selective agonists with intermediate potencies compared with homodimers, likely due to positive allostery between liganded partners in the homodimer. These results suggest that activation of heterodimers as well as of the receptor homodimer(s) targeted by the selective ligand needs to be considered in cells expressing both receptor types. Further, the robustness of the BRETFect signal indicates the applicability of these assays to high-throughput screens for drugs specifically targeting ER heterodimer vs. homodimer species. Note that although transient transfection was used for the assays described in this manuscript, stable expression of fusion proteins from retroviral or lentiviral vectors would likely minimize variability during arrayed screens. In addition, clonal selection would ensure more homogeneous expression levels within cell populations and/or expression levels more comparable to those of the endogenous proteins. Use of a Tet-On bicistronic inducible system for the intermediate and acceptor would enable adjusting expression levels of these proteins with respect to the donor levels to reach the saturation part of the interaction curve. The donor may alternatively be produced via homologous recombination with CRISPR-Cas9–guided recombination to achieve expression levels closer to the endogenous protein, provided that these levels of expression are sufficient for signal detection. Note, however, that this approach would ideally require recombination of all alleles to prevent competition from unfused proteins for interaction with the intermediate and acceptor.

We also provide evidence that BRETFect can be used with other types of receptors and their effectors. Based on the known dimeric nature of GPCRs and their recently reported capacity to interact simultaneously with several effectors, we investigated the formation of ternary complexes involving the V2R vasopressin receptor. AVP-induced complexes between V2R dimers and βArr2 and between V2R, βArr2, and Gγ2 were readily detected using BRETFect, providing robust assays to study the assembly of multimeric complexes involving V2R in real time.

Finally, the capacity to measure in parallel binary and ternary interactions offers a wealth of information on the mechanisms and kinetics of ternary complex assembly, as illustrated for the progressive assembly of SUMO3 molecules on preassembled ERα homodimers, or for the AVP-induced βArr2 interaction with precoupled V2R–Gγ2.

In conclusion, BRETFect is a robust and broadly applicable method to monitor a variety of ternary complexes and enable the development of drugs targeting them, as illustrated here for ternary protein complexes assembled by nuclear receptors or GPCRs.

Materials and Methods

HEK293T cells were maintained and transfected via polyethyleneimine as described in *SI Materials and Methods*. BRETFect and SRET assay transfection mixes contained 100 ng of RLucII-tagged donor, with 400 ng of mTFP1-tagged (GFP2-tagged for SRET^2) intermediate and 1 μg of Venus-tagged acceptor (for 1.25 million cells). In BRETFect and SRET control reactions, the intermediate fusion protein was replaced by unfused ERα/β or V2R, or alternatively by the same receptors fused to mTagBFP2, to maintain the total concentration of receptor constant in the D + A controls, and the expression vector for the YFP acceptor fusion protein was replaced by the parental vector for unfused YFP (amounts adjusted to generate similar emission levels) to control for random collisions in the D + I controls. For spectral analysis of BRETFect, cells were transfected with 250 ng ERα-RLucII, 500 ng ERα-mTFP1 (or untagged ERα or ERα-mTagBFP2), and 750 ng CoA-Venus (or 750 ng unfused Venus). For BRETFect titration, levels of transfected ERα-mTFP1 remained constant at 400 ng while transfected amounts of CoA-Venus varied from 0 to 1 μg; alternatively, levels of CoA-Venus were kept constant at 1 μg and amounts of transfected ERα-mTFP1 or unfused ERα varied from 0 to 400 ng. DNA concentrations were kept constant with parental vectors. For BRET, BRETFect, and SRET^2 experiments, cells were plated at a density of 125,000 cells per well in 96-well plates. Forty-eight

hours after transfection, cells were washed with PBS and treated with specified ligands or vehicle (0.1% DMSO) and incubated at 37 °C for the specified amount of time. Readings were collected immediately after coelenterazine addition (5 μM) on a TriStar^2 Multireader LB 942 microplate reader (Berthold Technologies) using BP485/40 nm (CTOP) and LP550 nm (TTO) filters for BRETFect and BP400/70 nm (donor) and BP530/20 nm (acceptor) filters for SRET^2. Fluorescence readings and FRET assays were performed using a FlexStation II microplate reader (Molecular Devices) with excitation of mTFP1 at 420 nm and measuring emission of mTFP1 at 495 nm and of YFPs at 550 nm. Emission spectrum experiments were performed on a Synergy Neo microplate reader (BioTek) with 800,000 cells per well in suspension using 2-nm intervals from 400 to 600 nm (see also *SI Materials and Methods* for a description of BRETFect plasmids, reagents, and assays; BRETFect protocols can also be accessed at bioinfo.iric.ca/maderlab/protocols/BRETFect/).

ACKNOWLEDGMENTS. We thank Drs. J. H. White and P. Maddox for reviewing this article. This study was supported by grants from the Canadian Institutes for Health Research (to S.M., MOP125863; to E.G., MOP133726). D.C.W. was supported by a scholarship from the Fonds de Recherche du Québec-Santé (FRQS). M.B. holds the Canada Research Chair in Signal Transduction and Molecular Pharmacology. E.G. is recipient of an FRQS Junior 2 salary award. S.M. holds the Canadian Imperial Bank of Commerce Breast Cancer Research Chair.

1. Sun Y, Wallrabe H, Booker CF, Day RN, Periasamy A (2010) Three-color spectral FRET microscopy localizes three interacting proteins in living cells. *Biophys J* 99:1274–1283.
2. Pauker MH, Hassan N, Noy E, Reicher B, Barda-Saad M (2012) Studying the dynamics of SLP-76, Nck, and Vav1 multimolecular complex formation in live human cells with triple-color FRET. *Sci Signal* 5:rs3.
3. Rebois RV, et al. (2008) Combining protein complementation assays with resonance energy transfer to detect multipartner protein complexes in living cells. *Methods* 45: 214–218.
4. Carriba P, et al. (2008) Detection of heteromerization of more than two proteins by sequential BRET-FRET. *Nat Methods* 5:727–733.
5. Wong KA, O'Bryan JP (2011) Bimolecular fluorescence complementation. *J Vis Exp* (50):2643.
6. Luker GD, Luker KE (2011) Luciferase protein complementation assays for bioluminescence imaging of cells and mice. *Methods Mol Biol* 680:29–43.
7. Nilsson S, et al. (2001) Mechanisms of estrogen action. *Physiol Rev* 81:1535–1565.
8. Sanchez R, Nguyen D, Rocha W, White JH, Mader S (2002) Diversity in the mechanisms of gene regulation by estrogen receptors. *BioEssays* 24:244–254.
9. White JH, Fernandes I, Mader S, Yang XJ (2004) Corepressor recruitment by agonist-bound nuclear receptors. *Vitam Horm* 68:123–143.
10. Hall JM, McDonnell DP (2005) Coregulators in nuclear estrogen receptor action: From concept to therapeutic targeting. *Mol Interv* 5:343–357.
11. Shanle EK, Xu W (2010) Selectively targeting estrogen receptors for cancer treatment. *Adv Drug Deliv Rev* 62:1265–1276.
12. Matthews J, Gustafsson JA (2003) Estrogen signaling: A subtle balance between ER alpha and ER beta. *Mol Interv* 3:281–292.
13. Murphy LC, et al. (2005) Inducible upregulation of oestrogen receptor-beta1 affects oestrogen and tamoxifen responsiveness in MCF7 human breast cancer cells. *J Mol Endocrinol* 34:553–566.
14. Hodges-Gallagher L, Valentine CD, El Bader S, Kushner PJ (2008) Estrogen receptor beta increases the efficacy of antiestrogens by effects on apoptosis and cell cycling in breast cancer cells. *Breast Cancer Res Treat* 109:241–250.
15. Jordan VC (1997) Tamoxifen treatment for breast cancer: Concept to gold standard. *Oncology (Williston Park)* 11(2, Suppl 1):7–13.
16. Howell A, et al. (2002) Fulvestrant, formerly ICI 182,780, is as effective as anastrozole in postmenopausal women with advanced breast cancer progressing after prior endocrine treatment. *J Clin Oncol* 20:3396–3403.
17. Loening AM, Fenn TD, Wu AM, Gambhir SS (2006) Consensus guided mutagenesis of Renilla luciferase yields enhanced stability and light output. *Protein Eng Des Sel* 19: 391–400.
18. Nagai T, et al. (2002) A variant of yellow fluorescent protein with fast and efficient maturation for cell-biological applications. *Nat Biotechnol* 20:87–90.
19. Shaner NC, Steinbach PA, Tsien RY (2005) A guide to choosing fluorescent proteins. *Nat Methods* 2:905–909.
20. Ai HW, Henderson JN, Remington SJ, Campbell RE (2006) Directed evolution of a monomeric, bright and photostable version of *Clavularia* cyan fluorescent protein: Structural characterization and applications in fluorescence imaging. *Biochem J* 400: 531–540.
21. Yarbrough D, Wachter RM, Kallio K, Matz MV, Remington SJ (2001) Refined crystal structure of DsRed, a red fluorescent protein from coral, at 2.0-Å resolution. *Proc Natl Acad Sci USA* 98:462–467.
22. Subach OM, Cranfill PJ, Davidson MW, Verkhusha VV (2011) An enhanced monomeric blue fluorescent protein with the high chemical stability of the chromophore. *PLoS One* 6:e28674.
23. Savkur RS, Burris TP (2004) The coactivator LXXLL nuclear receptor recognition motif. *J Pept Res* 63:207–212.
24. Weatherman RV, et al. (2002) Ligand-selective interactions of ER detected in living cells by fluorescence resonance energy transfer. *Mol Endocrinol* 16:487–496.
25. Koterba KL, Rowan BG (2006) Measuring ligand-dependent and ligand-independent interactions between nuclear receptors and associated proteins using bioluminescence resonance energy transfer (BRET). *Nucl Recept Signal* 4:e021.
26. Lupien M, et al. (2007) Raloxifene and ICI182,780 increase estrogen receptor-alpha association with a nuclear compartment via overlapping sets of hydrophobic amino acids in activation function 2 helix 12. *Mol Endocrinol* 21:797–816.
27. Powell E, Xu W (2008) Intermolecular interactions identify ligand-selective activity of estrogen receptor alpha/beta dimers. *Proc Natl Acad Sci USA* 105:19012–19017.
28. Traboulsi T, El Ezzy M, Gleason JL, Mader S (2017) Antiestrogens: Structure-activity relationships and use in breast cancer treatment. *J Mol Endocrinol* 58:R15–R31.
29. Zwart W, et al. (2010) The hinge region of the human estrogen receptor determines functional synergy between AF-1 and AF-2 in the quantitative response to estradiol and tamoxifen. *J Cell Sci* 123:1253–1261.
30. Tremblay A, Tremblay GB, Labrie F, Giguère V (1999) Ligand-independent recruitment of SRC-1 to estrogen receptor beta through phosphorylation of activation function AF-1. *Mol Cell* 3:513–519.
31. Cotnoir-White D, Laperrière D, Mader S (2011) Evolution of the repertoire of nuclear receptor binding sites in genomes. *Mol Cell Endocrinol* 334:76–82.
32. Hilmi K, et al. (2012) Role of SUMOylation in full antiestrogenicity. *Mol Cell Biol* 32: 3823–3837.
33. Stauffer SR, et al. (2000) Pyrazole ligands: Structure-affinity/activity relationships and estrogen receptor-alpha-selective agonists. *J Med Chem* 43:4934–4947.
34. Meyers MJ, et al. (2001) Estrogen receptor-beta potency-selective ligands: Structure-activity relationship studies of diarylpropionitriles and their acetylene and polar analogues. *J Med Chem* 44:4230–4251.
35. Helguero LA, Faulds MH, Gustafsson JA, Haldosén LA (2005) Estrogen receptors alfa (ERalpha) and beta (ERbeta) differentially regulate proliferation and apoptosis of the normal murine mammary epithelial cell line HC11. *Oncogene* 24:6605–6616.
36. Paulmurugan R, Tamrazi A, Massoud TF, Katzenellenbogen JA, Gambhir SS (2011) In vitro and in vivo molecular imaging of estrogen receptor α and β homo- and heterodimerization: Exploration of new modes of receptor regulation. *Mol Endocrinol* 25:2029–2040.
37. Shiau AK, et al. (1998) The structural basis of estrogen receptor/coactivator recognition and the antagonism of this interaction by tamoxifen. *Cell* 95:927–937.
38. Yi P, et al. (2015) Structure of a biologically active estrogen receptor-coactivator complex on DNA. *Mol Cell* 57:1047–1058.
39. Zhang JH, Chung TD, Oldenburg KR (1999) A simple statistical parameter for use in evaluation and validation of high throughput screening assays. *J Biomol Screen* 4: 67–73.
40. Angers S, Salahpour A, Bouvier M (2002) Dimerization: An emerging concept for G protein-coupled receptor ontogeny and function. *Annu Rev Pharmacol Toxicol* 42: 409–435.
41. Ferré S, et al. (2014) G protein-coupled receptor oligomerization revisited: Functional and pharmacological perspectives. *Pharmacol Rev* 66:413–434.
42. Armando S, et al. (2014) The chemokine CXC4 and CC2 receptors form homo- and heterooligomers that can engage their signaling G-protein effectors and βarrestin. *FASEB J* 28:4509–4523.
43. Terrillon S, Bouvier M (2004) Receptor activity-independent recruitment of betaarrestin2 reveals specific signalling modes. *EMBO J* 23:3950–3961.
44. Thomsen ARB, et al. (2016) GPCR-G protein-β-arrestin super-complex mediates sustained G protein signaling. *Cell* 166:907–919.
45. Rebois RV, Warner DR, Basi NS (1997) Does subunit dissociation necessarily accompany the activation of all heterotrimeric G proteins? *Cell Signal* 9:141–151.
46. Klein S, Reuveni H, Levitzki A (2000) Signal transduction by a nondissociable heterotrimeric yeast G protein. *Proc Natl Acad Sci USA* 97:3219–3223.
47. Galés C, et al. (2006) Probing the activation-promoted structural rearrangements in preassembled receptor-G protein complexes. *Nat Struct Mol Biol* 13:778–786.
48. Bünemann M, Frank M, Lohse MJ (2003) Gi protein activation in intact cells involves subunit rearrangement rather than dissociation. *Proc Natl Acad Sci USA* 100: 16077–16082.
49. McKay JP, Raizen DM, Gottschalk A, Schafer WR, Avery L (2004) eat-2 and eat-18 are required for nicotinic neurotransmission in the *Caenorhabditis elegans* pharynx. *Genetics* 166:161–169.
50. Bacart J, Corbel C, Jockers R, Bach S, Couturier C (2008) The BRET technology and its application to screening assays. *Biotechnol J* 3:311–324.
51. Zimmermann T, Rietdorf J, Girod A, Georget V, Pepperkok R (2002) Spectral imaging and linear un-mixing enables improved FRET efficiency with a novel GFP2-YFP FRET pair. *FEBS Lett* 531:245–249.
52. Tremblay GB, Tremblay A, Labrie F, Giguère V (1999) Dominant activity of activation function 1 (AF-1) and differential stoichiometric requirements for AF-1 and -2 in the estrogen receptor alpha-beta heterodimeric complex. *Mol Cell Biol* 19:1919–1927.
53. Powell E, et al. (2012) Identification of estrogen receptor dimer selective ligands reveals growth-inhibitory effects on cells that co-express ERα and ERβ. *PLoS One* 7: e30993.